ELSEVIER

Carbohydrate Research 308 (1998) 173–179

Note

Thermodynamics of borate ester formation by three readily grafted carbohydrates

Bryan M. Smith, Jennifer L. Owens, Christopher N. Bowman, Paul Todd *

Department of Chemical Engineering, Campus Box 424, University of Colorado, Boulder, CO 80309-0424, USA

Received 15 October 1997; accepted in revised form 20 February 1998

Abstract

Borate ester association constants for D-*glycero*-D-*gulo*-heptonamide (**1**), *N*-methyl-D-glucamine (**2**), and disorbitylamine (**3**) were derived from ^{11}B NMR observations. Significant electrostatic effects were observed in the formation of borate esters with the ammonium derivative (**2**). ^{11}B NMR studies of **3** were consistent with the simultaneous formation of intramolecular tetradentate borate diesters and oligomeric chains of **3** connected by intermolecular borate diesters. The process enthalpies for formation of borate monoesters and diesters with **1** are $\Delta H_1^\circ = -37.2 \pm 4.9$ kJ/mol and $\Delta H_2^\circ = -19.6 \pm 2.5$ kJ/mol, respectively. The corresponding process entropies are $\Delta S_1^\circ = -51 \pm 17$ J/mol/K and $\Delta S_2^\circ = -28 \pm 8$ J/mol/K. © 1998 Elsevier Science Ltd. All rights reserved

Keywords: Borate esters; Thermodynamics; ^{11}B NMR; Intramolecular borate diesters; Electrostatic effects; Chelate polymer

From the rich and thorough literature on the formation of borate esters [1–10], it is apparent that borate esters form when the borate anion reacts with polyhydroxy compounds, as shown in Scheme 1. An affordable and efficient process for the removal and concentration of boric acid from aqueous solutions might be achieved by immobilizing certain inexpensive carbohydrates.

This paper reports on the borate ester association thermodynamics for D-*glycero*-D-*gulo*-heptonamide (**1**), *N*-methyl-D-glucamine (**2**) and disorbitylamine, bis(D-*gluco*-2,3,4,5,6-pentahydroxyhexyl)amine, (**3**). These inexpensive functional groups are shown below; they can be readily attached to a dissolved or solid polymer surface containing appropriate reactive groups. In the case of **1**, suitable polymer precursors would contain primary amines to allow the facile ring-opening coupling reaction of commercially available α-D-glucoheptonic-γ-lactone [11]. To attach amines **2** and **3** to functional polymers, the polymer precursor should contain alkyl halides [12] or epoxides. These functional groups, therefore, offer many possibilities in applications to boron removal and concentration, as well as possible synergistic metal ion sequestration [10].

The complexation equilibria in dissolved functional polymers strongly favors the formation of borate diesters (BL_2) over borate monoesters (BL),

* Corresponding author. Fax: 00 303 492 4341.

PII S0008-6215(98)00075-5

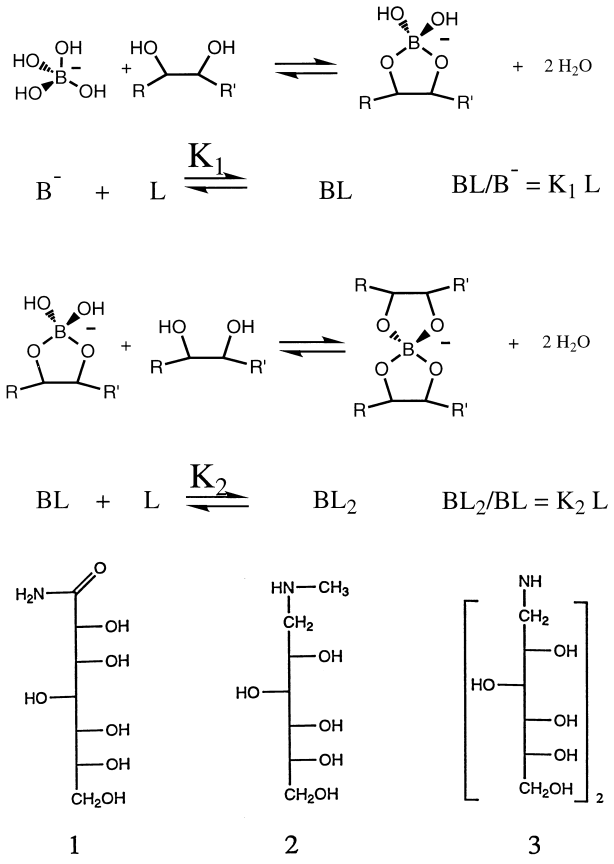

Scheme 1. Formation of borate esters and diesters with polyhydroxy compounds.

due to the high *local* concentration of chelating groups in the vicinity of a given borate monoester [7,12–14]. Since, on an atomic scale, the same borate ester structures are formed with both free functional groups (**1**–**3**) and the corresponding polymer-bound functional groups, the thermodynamics are expected to be quite similar between the two processes, with the exception of conformational entropy restrictions when **1**–**3** are attached to polymers. A promising model of polymer chelation has been proposed [14], and validation of this model requires independent measurement of the association constants of borate ester formation.

In this study, ^{11}B NMR was used to quantify the concentrations of the various boron species in solution. Borate diesters exhibit resonance peaks distinct from those of borate monoesters, and both are distinct from unbound boron as borate and boric acid. Therefore, with knowledge of the solution pH—to partition the unbound boron signal into boric acid and the active borate anion—and total boron and ligand concentrations, the actual species concentrations can be calculated from the NMR resonance peak areas and used to find the association constants. Fig. 1 shows a sample ^{11}B NMR spectrum of **2**, typical of those used in this study, with a sample deconvolution as discussed in the experimental section.

1. Results and discussion

D-Glycero-D-gulo-*heptonamide* (**1**).—At least four borate monoesters of **1** occur in aqueous solution, as peaks are observed corresponding [9] to two *erythro* complexes, one *threo* complex and one 1,3-diol complex. Since each of these peaks may actually arise from multiple species, and since their ^{11}B NMR peaks are distinguishable only at high pH, these individual signals were not studied independently. Instead, their intensities were summed, and distinction was made only between net borate monoesters and net borate diesters. Since we have not calculated individual species concentrations for the various esters, we therefore report overall association constants for the formation of borate monoesters and diesters according to the generalized reactions in Scheme 1, as is the convention in the literature [5,9]. While the process enthalpies and entropies reported do not describe individual discrete reactions, they are nonetheless useful for predicting the temperature dependence of borate ester formation, which is needed for practical applications.

The borate ester association constants, K_1 and K_2, were determined at 1°, 20° and 35 °C. Fig. 2 shows the ratios of borate monoesters to borate anion, and borate diesters to monoesters, both as a function of free ligand (**1**) concentration at 20 °C. It follows from Scheme 1 that, in Fig. 2a, K_1 is the slope of the best fit line passing through the origin. Similarly, K_2 is taken as the slope in Fig. 2b, where the ratio of borate diesters to borate monoesters is plotted as a function of free ligand concentration at 20 °C. These equilibrium experiments were repeated at 1° and 35°C.

The error bars in Figs 2–4 represent standard errors based on multiple fits to single ^{11}B NMR spectra. These uncertainties arise from the difficulty in properly phasing the broad and overlapping peaks under the experimental conditions. Since the free ligand concentration, $[L_f]$, is also calculated from the spectra, there is appreciable experimental uncertainty in this variable as reflected by the hori-

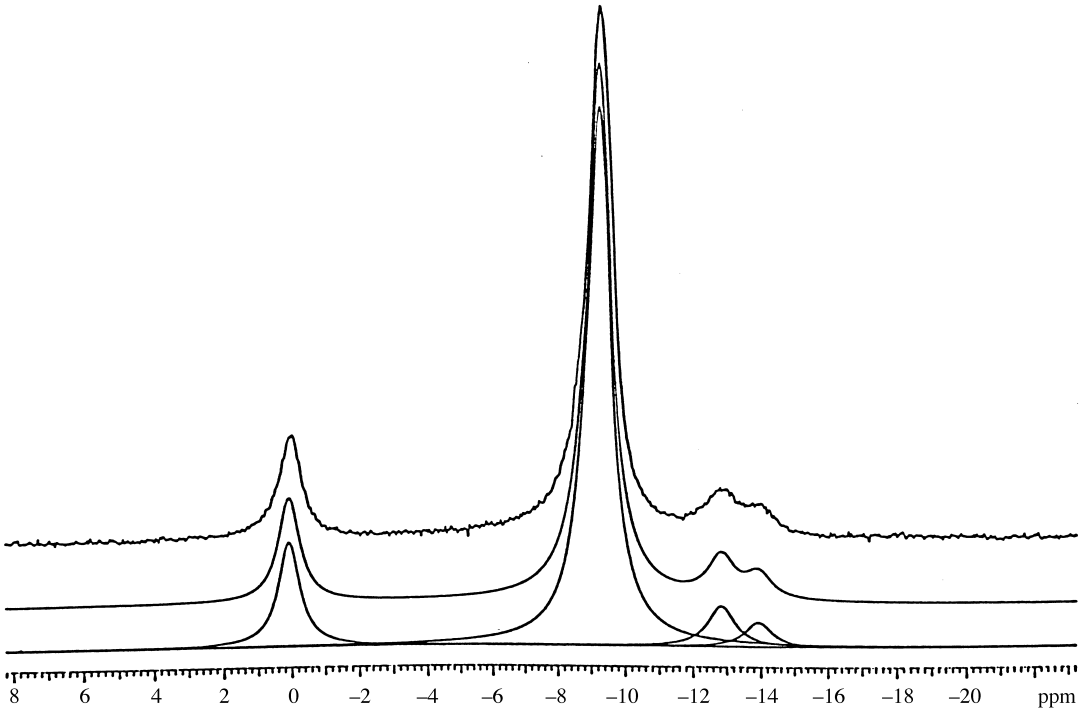

Fig. 1. ^{11}B NMR spectrum (top) of 0.050 M $B(OH)_3$ and 0.105 M **2** in H_2O at pH 6.25 and 21 °C. The lower traces are a deconvolution fit to the spectrum and the individual deconvoluted peaks. Chemical shifts are relative to boric acid and are externally referenced to sodium borate (pH 12) at −17.8 ppm. Peak assignments (from left to right) are: unbound boron (0.0 ppm), BL_2 diester (−9.2 ppm), BL *threo*-1,2,-monoester (−12.8 ppm), and BL *erythro*-1,2-monoester (−14.0 ppm) [9].

zontal error bars in Figs 2–4. These experimental uncertainties were not used to weight the least-squares fits which produce the values of the association constants and their standard errors.

Table 1 contains the values of association constants calculated at the three temperatures studied as well as the enthalpies and entropies of association derived from them. Not surprisingly, the association constants reported here agree well with those reported for D-mannitol and D-glucitol [5], and the thermodynamic parameters are in general agreement with those determined for other borate esters [7,15–17].

N-*Methyl*-D-*glucamine* (**2**).—Fig. 3a shows that the solution pH strongly affects the apparent association constant, K_1, between borate and **2**. It is likely that the electrostatic attraction between the protonated amines (pH 6.0–8.5) and their anionic borate esters stabilizes the complexes by the observed 2.7 kJ/mol relative to the unprotonated amines (pH > 11.5). A pH dependence is not observed in diester formation (Fig. 3b), presumably because one of the reacting components is neutral at all pH values. A previous report [12] of the borate association constants of **2** neglected this apparent electrostatic effect on K_1 and used an incomplete reaction model which resulted in unreasonably high estimates of K_2.

Disorbitylamine (**3**).—This functional group is of particular interest as it appears to offer the possibility of tetradentate chelation. In a borate removal system, this structure of borate diester would reduce intermolecular borate crosslinking in soluble polymers and improve extraction efficiency at low boron concentrations in solid polymers. A previous study [10] suggested that, based on the unusually broad peak-width of the ^{11}B NMR signal from the borate diester of **3**, a crown- or cryptand-type structure in which two borate diesters bridge two disorbitylamine molecules is more likely. This analysis neglects two possibilities. It is possible, though unlikely based on ^{13}C NMR data [10] on the borate esters of **3** and similar compounds, that two or more distinct borate diester species are formed, each having a different ^{11}B NMR chemical shift. The borate diester peaks are so broad that two such overlapping peaks would be indistinguishable from one broad peak. Another possibility is that the borate diesters of **3** are non-specific oligomers, containing several disorbitylamine molecules bridged by borate diesters. These large species would also account for

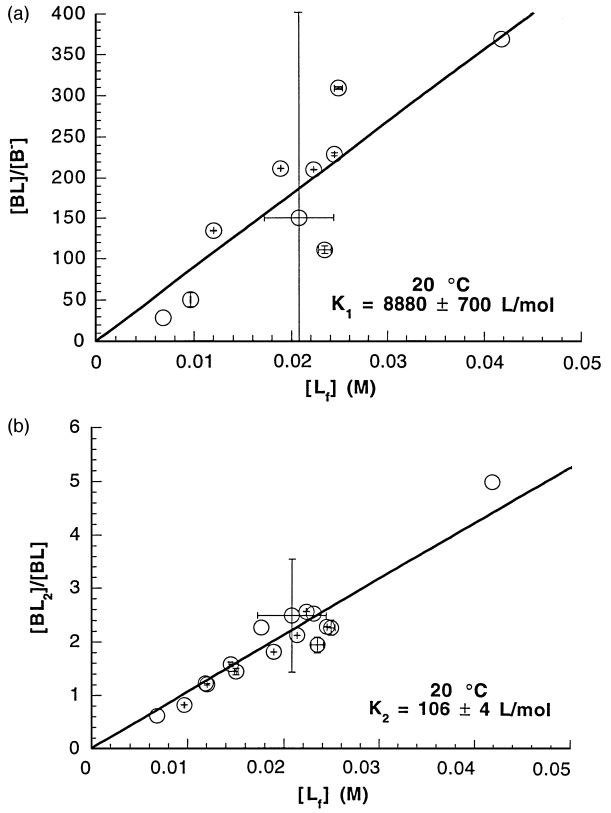

Fig. 2. Equilibria of borate monoester (a) and diester (b) formation with **1**, 20 °C. Total boron concentration was maintained below 0.05 M and pH ranged from 6.0 to 8.5. Standard errors in both independent and dependent variables result from the difficulty in unambiguously phasing the NMR spectra as described in the text.

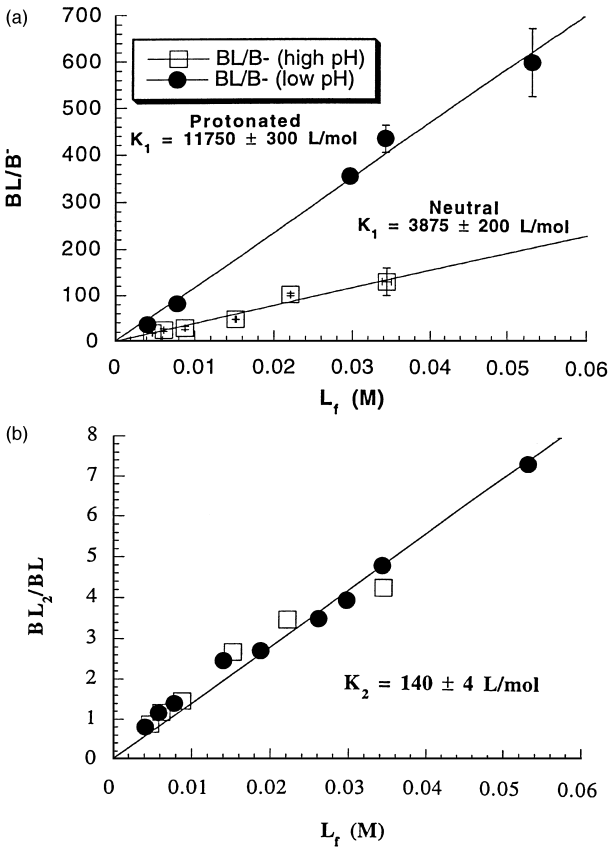

Fig. 3. Equilibria of borate monoester (a) and diester (b) formation with **2**, 21 °C. Total boron concentration was maintained below 0.05 M. The samples labeled as high pH (□) were pH > 11.5; low pH samples (●) were pH 6.0–8.5. Standard errors in both independent and dependent variables result from the difficulty in unambiguously phasing the NMR spectra.

the unusually broad borate diester peaks observed.

To produce Fig. 4, we assume that the unbound functional group concentration, $[L_f]$, is defined by the concentration of free sorbityl groups ($[L_f]=2\times[\mathbf{3}]-2\times[BL_2]-[BL]$). This approach is supported by the fact that the contrary assumption, that each molecule of **3** is able to bind only one borate anion, leads to negative calculated concentrations of unbound **3**. Also, both the observed ratios of borate monoester to borate anion and the ratios of borate diester to monoester do not scale linearly with the calculated concentration of free **3**, but only with the calculated concentration of free sorbityl groups. Our assumption that the sorbityl groups react independently neglects the possible electrostatic repulsion between borate monoesters on a single molecule of **3** and presumably accounts for some of the scatter in Fig. 4a.

Note that in Fig. 4b, the ratio of borate diesters to monoesters clearly does not extrapolate to zero at low $[L_f]$. This result is consistent with tetradentate chelation if one considers the formation of a tetradentate complex (LBL) from a monoborate monoester of disorbitylamine (BLL, where LL designates the disorbitylamine molecule with its two ligand sites):

$$\mathrm{BLL} \xleftrightarrow{K_3} \mathrm{LBL} \qquad (1)$$

It is assumed that two borate monoesters may form with one molecule of **3**, $\mathrm{BLL}+\mathrm{B}^-\leftrightarrow\mathrm{BLLB}$, but that the reaction of the tetradentate diester with borate, $\mathrm{LBL}+\mathrm{B}^-\leftrightarrow\mathrm{BLBL}$, does not occur. The concentration of the monoborate monoester species, [BLL], may be approximated by calculating the probability that two ligands contain only one borate monoester between them, assuming that the sorbityl branches react independently, with identical equilibria:

$$[\mathrm{BLL}] = 2\times\frac{[\mathrm{BL}]}{[L_t]}\times\frac{[L_f]}{[L_t]}\times\frac{[L_t]}{2} = [\mathrm{BL}]\times\frac{[L_f]}{[L_t]} \qquad (2)$$

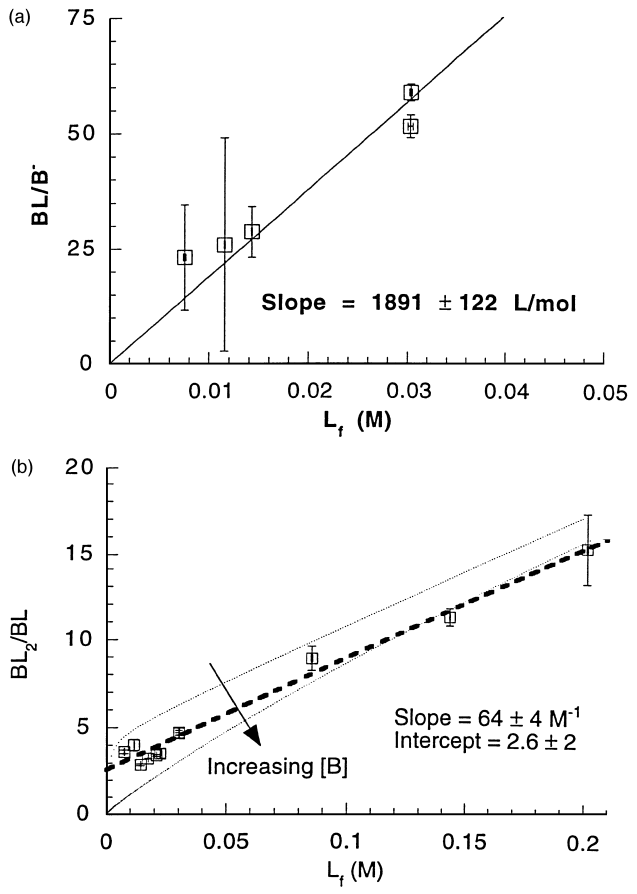

Fig. 4. Equilibria of borate monoester (a) and diester (b) formation with **3**, 21 °C. Total boron concentration was maintained below 0.05 M and pH was above 11.5. (a) Observed borate monoester formation with free sorbityl groups of **3**. (b) Borate diester formation: the dashed line is the linear least-squares fit to the observed data. The other two curves are predicted ratios of $[BL_2]/[BL]$ from the reaction model described in the text, with $K_2 = 63.5\,M^{-1}$, $K_3 = 4.5$ and total boron concentrations of 0.5 and 50 mM. The boron concentrations modeled include the entire experimental range, and the data points at higher $[L_f]$ resulted from solutions with boron concentrations to the high end of that range. Standard errors in both independent and dependent variables result from the difficulty in unambiguously phasing the NMR spectra.

The equilibrium concentration of total borate diesters now reduces to

$$[BL_2] = K_2 \times [BL] \times [L_f] + K_3 \times [BL] \times \frac{[L_f]}{[L_t]} \quad (3)$$

and a plot of $[BL_2]/[BL]$ versus $[L_f]$ may be approximated by a straight line if $[L_f/L_t]$ is nearly constant or K_3 is small. In our samples, the calculated ratio of $[L_f/L_t]$ ranges from 0.25 to 0.7 with a mean of 0.48. Simplifying eq (3) by substituting this mean value leads to an estimate of $K_3 = 5.4$ from the intercept of Fig. 4b.

Alternatively, one may create a family of curves of $[BL_2]/[BL]$ versus $[L_f]$ with total borate concentration as the parameter by simultaneously solving the mass balances on functional groups and boron subject to the equilibrium expressions for borate monoester and total diester formation. Fig. 4b shows that the family of such curves, with total boron concentrations spanning the experimentally investigated range, brackets the observations. This reaction model also allows for the formation of oligomeric species in which borate diesters bridge several molecules of **3**, and these species would account for the unusually broad ^{11}B NMR linewidths previously observed [10]. Fig. 5 shows the predicted ratios of borate diesters to monoesters, calculated from eq (3), compared to the observed ratios, and it is clear that the observations parallel the predictions. We therefore conclude that the simple reaction model incorporating both intramolecular tetradentate borate diesters and, perhaps more importantly, oligomeric borate diesters of **3** adequately describes these ^{11}B NMR observations, as well as previous reports in the literature, when the value of K_3 is 4–5. While these observations cannot exclude other structural possibilities, the fact that Fig. 4b is essentially linear in free sorbityl group concentration argues strongly for the existence

Table 1
Thermodynamics of borate ester formation with **1**

Reaction	T (°C)	K (L/mol) [a]	$\Delta H°$ (kJ mol^{-1}) [a,b]	$\Delta S°$ (J mol^{-1} K^{-1}) [a,b]
$B + L \Longleftrightarrow BL$	1	29 900 ± 5400	−37.2 ± 4.9	−51 ± 17
	20	8900 ± 700		
	35	5200 ± 1000		
$BL + L \Longleftrightarrow BL_2$	1	189 ± 18	−19.6 ± 2.5	−28 ± 8
	20	106 ± 4		
	35	73 ± 6		

[a] Uncertainties are standard errors of the fitted parameters.
[b] Derived from a least-squares fit, weighted by the uncertainties in ln (K) values, to the van't Hoff relationship: $\ln(K) = (-\Delta H/R)(1/T) + \Delta S/R$.

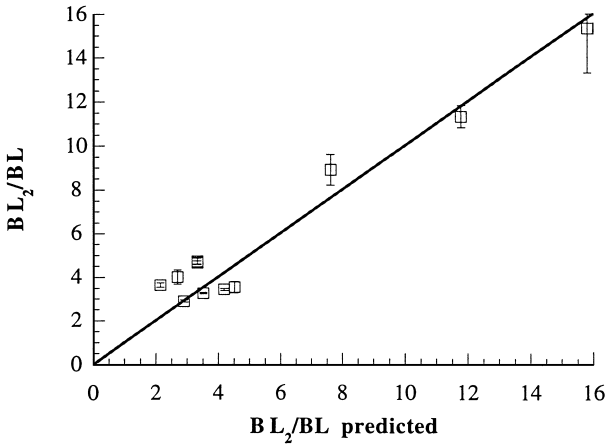

Fig. 5. Observed versus predicted ratios of borate diesters to borate monoesters for the disorbitylamine–borate system. The solid line is of the form $y = x$ for comparison. Predicted ratios were based on simultaneous solution of mass balances on boron and ligand with borate diester equilibria described by eq (3) with $K_1 = 1891\ M^{-1}$, $K_2 = 63.5\ M^{-1}$ and $K_3 = 4.5$.

of oligomers of **3** in which the sorbityl branches are bridged by at least one structurally distinct type of borate diester.

2. Experimental

D-Glycero-D-gulo-*heptonamide* (**1**).—α-D-Gluco-heptonic-γ-lactone (5.0 g, 24.0 mmol) (Aldrich) was dissolved in 50 mL Me_2SO (Malinkrodt) which had been predried over 3 Å molecular sieves (Aldrich). This solution was maintained at 40 ± 1 °C throughout the reaction. Ammonia gas was generated by warming aqueous NH_4OH and condensing the water vapor in a coldtrap maintained at −20 ± 10 °C. The dry ammonia gas was bubbled through the Me_2SO solution for 11.5 h. Without further purification, solvent was removed by rotary evaporation with a convective flow of dry N_2 for 10 d to give a white solid, over 99% pure by ^1H NMR: mp 120–122°C (dec), lit. [18] 134.5 °C; $[\alpha]_D$ +9.76° (*c* 1.45, H_2O), lit. [18] $[\alpha]_D$ +10.6°; IR (KBr): ν 1657 (amide C=O stretch) and 1592 cm^{-1} (amide N–H bend); ^1H NMR (Me_2SO-d_6): δ 7.31 (s, 2 H), 5.46 (d, 1 H), 4.88 (d, 1 H), 4.49 (d, 1 H), 4.47 (d, 1 H), 4.40 (d, 1 H), 4.32 (t, 1 H), 3.87 (m, 2 H), 3.65 (ddd, 1 H), 3.54 (ddd, 1 H), 3.45 (m, 2 H), 3.36 (m, 1 H); ^{13}C NMR (Me_2SO-d_6): δ 175.93, 74.55, 73.57, 71.76, 71.46, 67.96, 63.28; MS (electrospray): *m*/*z* 226 ($M+H^+$); Anal. Calcd for $C_7H_{15}NO_7$: C, 37.3; H, 6.7; N, 6.2; O, 49.7. Found (Huffman Laboratories, Golden, CO): C, 37.3; H, 6.5; N, 6.2; O, 51.4.

General.—Samples of amines **2** and **3** (Aldrich) were obtained commercially and used without further purification. IR spectra were recorded in KBr matrix on a Nicolet 750 FTIR at 0.5 cm^{-1} resolution. Samples for ^{11}B NMR analysis were prepared in 1 mL volumetric flasks from stock solutions of boric acid (Fisher, electrophoresis grade) and the given complexing agent. After adjusting the pH with HCl or NaOH, samples were diluted to final volume, and final pH values were measured in the flasks with an Orion PerpHect 300 meter and a narrow Cole-Parmer probe (H-05990-30) calibrated at the appropriate temperature. In all cases, the boron concentration was kept below 0.05 M to minimize polyborate formation, and the ratio of complexing agent to boron was kept above 2.05 (1.1 for **3**) to minimize polyborate ester formation [5,12] (e.g. B_2L species). All NMR spectra were recorded on a Varian VXR-300S with a boron-free insert. To avoid interference from broad boron background signals, quartz tubes were used for samples with low boron concentrations. Sample temperature was controlled within 0.1 °C (1.0 °C for samples at 20° and 21 °C) and samples were allowed to equilibrate for 10 min prior to signal acquisition. Due to the broad and overlapping resonances, ^{11}B NMR spectra were manually phased and the resonance peaks were fitted using the Varian deconvolution routine.

References

[1] C.F. Bell, R.D. Beauchamp, and E.L. Short, *Carbohydr. Res.*, 185 (1989) 39–50.
[2] S. Chapelle and J.-F. Verchere, *Tetrahedron*, 44 (1988) 4469–4482.
[3] J.G. Dawber and S.I.E. Green, *J. Chem. Soc. Faraday Trans. I*, 82 (1986) 3407–3413.
[4] J.G. Dawber, *J. Chem. Soc. Faraday Trans. I*, 83 (1987) 771–777.
[5] M. Makkee, A.P.G. Kieboom, and H. van Bekkum, *Recl. Trav. Chim. Pays-Bas*, 104 (1985) 230–235.
[6] T.L. Paál, *Acta Chim. Acad. Sci. Hung.*, 103 (1980) 181–191.
[7] S.W. Sinton, *Macromolecules*, 20 (1987) 2430–2441.
[8] R. van den Berg, J.A. Peters, and H. van Bekkum, *Carbohydr. Res.*, 353 (1994) 1–12.
[9] M. van Duin, J.A. Peters, A.P.G. Kieboom, and H. van Bekkum, *Tetrahedron*, 41 (1985) 3411–3421.
[10] J. van Haveren, H. Lammers, J.A. Peters, J.G. Batelaan, and H. van Bekkum, *Carbohydr. Res.*, 243 (1993) 259–271.

[11] K. Aoi, K. Itoh, and M. Okada, *Macromolecules*, 28 (1995) 5391–5393.
[12] B.M. Smith, P. Todd, and C.N. Bowman, *Sep. Sci. Technol.*, 30 (1995) 3849–3859.
[13] E. Pezron, L. Liebler, A. Ricard, F. Lafuma, and R. Audebert, *Macromolecules*, 22 (1988) 1169–1174.
[14] E.T. Wise and S.G. Weber, *Macromolecules*, 21 (1988) 8321–8327.
[15] E. Pezron, L. Liebler, A. Ricard, and R. Audebert, *Macromolecules*, 21 (1988) 1126–1131.
[16] R.D. Pizer, P.J. Ricatto, and C.A. Tihal, *Polyhedron*, 12 (1993) 2137–2142.
[17] J.M. Conner and V.C. Bulgrin, *J. Inorg. Nucl. Chem.*, 29 (1967) 1953–1961.
[18] C.S. Hudson and S. Komatsu, *J. Am. Chem. Soc.*, 41 (1919) 1141–1147.